Ca²⁺, NAD(P)H and membrane potential changes in pancreatic β-cells by methyl succinate: comparison with glucose

Emma HEART*†, Gordon C. YANEY*, Richard F. CORKEY*, Vera SCHULTZ*‡, Esthere LUC*, Lihan LIU*, Jude T. DEENEY*,
Orian SHIRIHAI§, Keith TORNHEIM*‡, Peter J. S. SMITH† and Barbara E. CORKEY*‡[1]

*Obesity Research Center, Evans Department of Medicine, Boston University School of Medicine, Boston, MA 02118, U.S.A., †BioCurrents Research Center, Marine Biological
Laboratory, Woods Hole, MA 02543, U.S.A., ‡Department of Biochemistry, Boston University School of Medicine, Boston, MA 02118, U.S.A., and §Department of Pharmacology and
Experimental Therapeutics, Tufts University School of Medicine, Boston, MA 02118, U.S.A.

The present study was undertaken to determine the main metabolic secretory signals generated by the mitochondrial substrate MeS (methyl succinate) compared with glucose in mouse and rat islets and to understand the differences. Glycolysis and mitochondrial metabolism both have key roles in the stimulation of insulin secretion by glucose. Both fuels elicited comparable oscillatory patterns of Ca²⁺ and changes in plasma and mitochondrial membrane potential in rat islet cells and clonal pancreatic β-cells (INS-1). Saturation of the Ca²⁺ signal occurred between 5 and 6 mM MeS, while secretion reached its maximum at 15 mM, suggesting operation of a K_{ATP}-channel-independent pathway. Additional responses to MeS and glucose included elevated NAD(P)H autofluorescence in INS-1 cells and islets and increases in assayed NADH and NADPH and the ATP/ADP ratio. Increased NADPH and ATP/ADP ratios occurred more rapidly with MeS, although similar levels were reached after 5 min of exposure to each fuel, whereas NADH increased more with MeS than with glucose. Reversal of MeS-induced cell depolarization by Methylene Blue completely inhibited MeS-stimulated secretion, whereas basal secretion and KCl-induced changes in these parameters were not affected. MeS had no effect on secretion or signals in the mouse islets, in contrast with glucose, possibly due to a lack of malic enzyme. The data are consistent with the common intermediates being pyruvate, cytosolic NADPH or both, and suggest that cytosolic NADPH production could account for the more rapid onset of MeS-induced secretion compared with glucose stimulation.

Key words: β-cell, calcium oscillation, insulin secretion, NADPH, membrane potential, metabolism.

INTRODUCTION

The pancreatic β-cell possesses a unique signal transduction system dependent on metabolism of fuel stimuli to initiate insulin secretion, and mitochondrial metabolism plays an important role in this process [1,2]. Reducing equivalents are supplied to the respiratory chain, where they are oxidized, resulting in ATP synthesis and a subsequent rise in the cytosolic ATP/ADP ratio. Increases in the ATP/ADP ratio are thought to close ATP-sensitive K⁺ channels (K_{ATP} channels), resulting in β-cell plasma membrane depolarization, activation of voltage-gated Ca²⁺ channels and Ca²⁺ influx [3]. Elevation of intracellular Ca²⁺ promotes insulin granule exocytosis [3]. Cytosolic Ca²⁺ rise is necessary for secretion, but is not sufficient to account for increased insulin secretion during a graded glucose challenge [4]. Other factors/messengers are required to explain graded insulin secretion with increasing fuel concentrations when the Ca²⁺ signal is saturated; this process is called the K_{ATP}-channel-independent pathway [5,6].

Another particular characteristic of glucose signalling in the β-cell is the generation of oscillations in metabolism, membrane potential, intracellular Ca²⁺ and, ultimately, secretion. It has been proposed that these oscillations are driven by glycolytic oscillations based on the unique characteristics of the key glycolytic enzyme PFK (phosphofructokinase) [7,8]. The importance of oscillations is based in part on observations of the greater potency of pulsatile insulin and of the loss of oscillatory secretion in patients with diabetes [9].

In addition to glucose, there are fuels that stimulate insulin secretion through mitochondrial metabolism [10]. Succinate, supplied as its membrane-permeant methyl ester (MeS), is metabolized efficiently [11] and potently stimulates insulin secretion [12,13] while bypassing glycolysis. The mechanism by which MeS generates the signals to stimulate secretion has not been established. Succinate, generated from MeS in the cytosol by esterases, enters the mitochondria in exchange for malate, which is then converted in the cytosol into pyruvate by malic enzyme [14]. Pyruvate can then re-enter the tricarboxylic acid cycle [11,15]. Both pyruvate formation and anaplerosis [16] are considered to be critical factors for insulin secretion. Pyruvate generates both the acetyl-CoA needed for ATP production and the oxaloacetate needed for anaplerosis. In contrast with glucose, MeS stimulates insulin secretion in rat, but not in mouse, islets [17], a fact possibly explained by the absence of malic enzyme in mouse islets [17].

In the present study, we evaluated different metabolic aspects of MeS in comparison with glucose. The rise in NADPH, an early signal generated by MeS, preceded insulin secretion, suggesting the possible importance of the cytosolic NADPH/NADP ratio in MeS-induced insulin secretion. Additionally, secretion was increased further at higher stimulatory MeS concentrations, while Ca²⁺ did not increase further, suggesting a K_{ATP}-channel-independent component of MeS-induced secretion similar to glucose. Production of pyruvate and NADPH appear to be common features of stimulatory fuels.

Biochemical Journal

MATERIALS AND METHODS

Materials

Monomethyl succinate, FCCP (carbonyl cyanide *p*-trifluoro-methoxyphenylhydrazone) and rotenone were from Sigma–Aldrich.

Islet isolation and primary cell culture

Pancreatic islets were isolated from Sprague–Dawley rats or Swiss–Webster mice (Charles River) by collagenase digestion as described previously [4]. Islets were picked by hand four times under a dissecting microscope and then dispersed by incubation in Ca^{2+}/Mg^{2+}-free PBS containing 3 mM EGTA and 0.05 mg/ml trypsin for 10 min at 37 °C with occasional agitation. Isolated cells were centrifuged at 220 *g* for 4 min, washed and suspended in RPMI 1640 culture medium (Sigma) supplemented with 5 mmol/l glucose, 10 % fetal calf serum (HyClone), 100 IU/ml penicillin and 100 μg/ml streptomycin. A 100 μl aliquot containing an estimated 1×10^5 cells was plated on a 35 mm coverslip in a Petri dish (MatTek). Cells were allowed to adhere for 2 h before replenishment with 2 ml of RPMI 1640 medium containing 5 mmol/l glucose and 10 % fetal bovine serum. Experiments were performed on individual cells not in contact with other cells after culture for 2–3 days. Under these conditions, β-cells constituted approx. 75 % of the total cell content, as determined by infecting cells with insulin-promoter-directed green fluorescent protein [18]. Relatively large cells were selected for study, since, in mice, β-cells are known to be larger than α- and δ-cells [19].

INS-1 cell culture

INS-1 cells were maintained and cultured as described previously [20]. Before experiments, cells were dislodged by trypsin treatment (0.017 % trypsin with EGTA) and suspended in KRB (Krebs–Ringer bicarbonate) buffer containing 140 mmol/l NaCl, 30 mmol/l Hepes, 4.6. mmol/l KCl, 1 mmol/l $MgSO_4$, 0.15 mmol/l Na_2HPO_4, 0.4 mmol/l KH_2PO_4, 5 mmol/l $NaHCO_3$ and 2 mmol/l $CaCl_2$, pH 7.4, supplemented with 2 mmol/l glucose and 0.05 % BSA.

Fura 2 loading and Ca^{2+} measurement

Cells were loaded for 30 min at 37 °C with 0.5 μmol/l fura 2/AM (acetoxymethyl ester) (Molecular Probes) in KRB buffer containing 5 mmol/l glucose and 0.05 % BSA. After loading, cells were washed twice and incubated in this buffer for 15 min to allow cleavage of intracellular fura 2/AM by cytosolic esterases. The intracellular Ca^{2+} was measured by placing the dish containing cells on the stage of a Zeiss IM 35 inverted microscope using a 40× glycerine objective in a temperature-controlled cabinet heated to 37 °C. Intracellular fura 2 was excited using a xenon lamp and a dual-wavelength Ionoptix synchronized chopper mirror at 340 and 380 nm. Fluorescence excitation intensity at 380 nm was equalized with that at 340 nm using a neutral-density filter. The fura 2 emission signal at 510 nm was recorded by an intensified CCD (charge-coupled device) Ionoptix camera. Images were collected at 4 s intervals. Fluorescence data were acquired and analysed using Ion Wizard software (IonOptix). The free Ca^{2+} concentration was calculated from the fluorescence ratio R as described by Grynkiewicz et al. [21]. R_{max} and R_{min} were obtained by exposing cells to ionomycin or EGTA respectively [22]. A K_d of 224 nmol/l for Ca^{2+} binding to free fura 2 [22] was used in calculations.

Membrane potential

To measure plasma membrane potential, cells were loaded with the potential-sensitive dye DiSBAC2(3) [bis-(1,3-diethyl-thiobarbituric acid) trimethine oxonol] (Molecular Probes) at 5 nmol/l (535 nm excitation/570 nm emission) in the same buffer as described for Ca^{2+} measurement. After dye addition, cells were allowed to equilibrate for 20 min. Images were obtained using the Ionoptix Fluorescence System interface, Dual Excitation Light Source, and intensified CCD camera coupled to a Zeiss IM35 inverted microscope. Temperature was maintained at 37 °C within a heated Faraday cage. The light source was a 150–200 W xenon short-arc lamp transmitted by a liquid light pipe. Chroma Filters used included 535/40× excitation, Q565DCXR dichroic and HQ610/75m emission. Signal output from the camera was recorded and analysed using Ion Wizard software.

To measure mitochondrial membrane potential, mitochondria were labelled using the mitochondria-specific dye TRME (tetra-methylrhodamine ethyl ester perchlorate) (Molecular Probes). Cells were incubated for 45 min before visualization in KRB buffer containing 10 nM TMRE. Confocal microscopy was performed on living cells using a Zeiss LSM510 microscope equipped with a heated stage with the HeNe (543 nm) and Ar (488 nm) lasers. The membrane-potential-dependent component of TMRE accumulates in a Nernstian fashion that can be described by the intensity of its fluorescence [4]. Values are expressed as arbitrary intensity units of TMRE fluorescence, using MTG (MitoTracker Green) to normalize the TMRE signal for the plane focal changes and based on basal values of 100 %.

NAD(P)H and NAD(P) measurements

INS-1 cell autofluorescence

Nicotinamide nucleotide fluorescence (340 nm excitation/420 nm emission) was measured in a suspension of INS-1 cells (10^6 cells/ml) using an Hitachi F 2000 fluorescence spectrophotometer. Cells, placed in a cuvette positioned inside a temperature-controlled chamber, were stirred during the experiment to ensure proper mixing. FCCP (1 μmol/l) and rotenone (1 μmol/l) were used to determine minimal and maximal reduction of nicotinamide nucleotides respectively.

Whole-islet autofluorescence

Freshly isolated mouse or rat islets were allowed to adhere overnight to Cell-Tak™-coated coverslips of 35 mm confocal dishes (MatTek) and then imaged on a Zeiss LSM510 confocal microscope equipped with a heated stage, using two-photon excitation of NAD(P)H as described previously [23]. NAD(P)H was excited by 150 fs pulses of 710-nm light from a Mira laser focused through a 40× objective [NA (numerical aperture) 1.3]. The excitation power was kept below 2.5 mW at the objective, to avoid photodamage to the islets. Autofluorescence was collected through a 380–550 custom-made Chroma filter [23]. Images were collected every 30 s. Minimal and maximal values were obtained by exposing islets to 3 μmol/l FCCP and 3 mmol/l NaN_3 respectively.

Enzymatic measurement of NADH and NADPH

Batches of 50–70 islets were incubated with fuels for 1 or 5 min and then extracted with 0.04 mmol/l NaOH and 0.5 mmol/l cysteine [24], vortex-mixed and sonicated for 15 s on ice. An aliquot was heated at 60 °C for 10 min to destroy NAD and NADP,

and the levels of NADH and NADPH were determined separately by enzymatic recycling method**s** [24], with modifications for NADH [25]. Levels of NADH + NAD and NADPH + NADP were measured in non-heated aliquots and corrected for the small amount of degradation (10 % or less) of NAD and NADP in cold alkali, using corresponding standards processed in parallel. Results are presented as the ratio between the amount of the reduced form and total, i.e. NADH/(NADH + NAD) and NADPH/(NADPH + NADP).

Insulin secretion

Glucose-stimulated insulin secretion was determined in perifused islets or in static incubations of dispersed cells. Dispersed islet cells were cultured in 48-well plates and stimulated with various glucose concentrations under the same conditions as described for Ca²⁺ studies. The amount of released insulin was determined after 30 min of static incubation with a radioimmunoassay kit (Linco Research) using rat insulin as the standard. For perifusion, batches of 50–80 islets were sandwiched between two layers of Cytodex-3 microcarrier beads in a 1 cm×1.5 cm column and perifused with KRB supplemented with 0.05 % BSA and 10 mM MeS at 37 °C as described previously [26].

ATP/ADP measurements

Batches of seven to ten islets were incubated with fuels for 1–5 min and deproteinized with 1 % trichloroacetic acid. After ether extraction, the samples were dried down and stored frozen at −80 °C. Samples were dissolved in 0.2 ml of water, and the ATP/ADP ratio was measured bioluminometrically using a Turner Model 20e luminometer equipped with a Cavro injector as described previously [27]. In this method, ADP is converted into ATP to be assayed by luciferase, after the sample is depleted of endogenous ATP with ATP sulfurylase, thus enhancing the sensitivity of the ADP measurement. Data are presented as the ATP/ADP ratio, making them independent of differences in cell number or loss of sample volume during extraction.

Malic enzyme activity

Islets (100) or clonal cells (2×10^6) were solubilized in 100 μl of protein-extraction reagent supplemented with a protease inhibitor cocktail (Pierce). After centrifugation at $14\,000\,\mathbf{g}$ for 15 min, supernatants were collected, stored at −20 °C and used for determination of malic enzyme activity. Protein extract (20 μg) or NADPH standard (1–100 nmol) was added to the reaction buffer (50 mM Hepes, pH 7.4, 1 mM NADP, 5 mM malate and 10 mM MnCl$_2$), in a stirred cuvette positioned inside a temperature-controlled chamber. Fluorescence was measured at 340 nm excitation and 460 nm emission on a FluoroMax-3 fluorescence spectrophotometer. A calibration curve was generated using known amounts of NADPH (product) in the sample buffer [28].

RESULTS

MeS effects on Ca²⁺ and insulin secretion

Figure 1 illustrates single rat and mouse islet cell Ca²⁺ responses to glucose and MeS. In rat islet cells, the period and peak (amplitude) of the Ca²⁺ oscillatory responses were similar with each fuel (Figures 1A and 1B), although there was a significantly shorter lag after fuel addition with MeS (69 ± 8 s; $n = 58$) compared with glucose (110 ± 23 s; $n = 45$, $P < 0.05$). MeS failed to increase
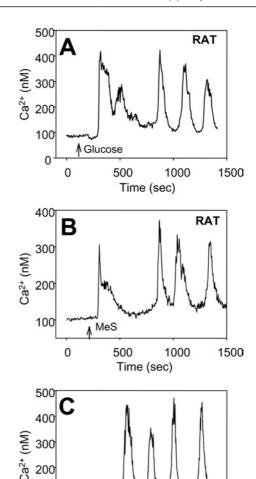

Figure 1 Ca²⁺ responses of rat and mouse islet cells to MeS and glucose
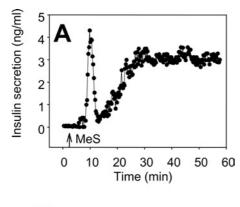
Glucose or MeS were raised from basal glucose (4 mmol/l) to 10 mmol/l at the times indicated by arrows. (**A**) Example of rat islet cell response to glucose ($n = 45$). (**B**) Example of rat islet cell response to MeS ($n = 58$). (**C**) Example of mouse islet cell response to glucose but not to MeS ($n = 65$).

Ca²⁺ in mouse islet cells. The absence of a mouse islet cell response to MeS, despite a Ca²⁺ response to subsequent glucose addition, is illustrated in Figure 1(C).

MeS-dependent insulin secretion from dispersed rat islet cells and perifused rat islets in response to MeS is shown in Figure 2. Similarly to glucose, MeS-elicited a biphasic secretory response in whole rat islets perifused in a column (Figure 2A). Insulin secretion was also studied in static incubations of dispersed rat islet cells under conditions similar to those used for the Ca²⁺ measurements. Interestingly, there was a difference in the MeS concentration-dependence for these processes. Whereas average Ca²⁺ values reached a maximum between 6 and 8 mmol/l MeS, insulin secretion continued to increase with higher MeS concentrations (Figure 2B).

Effect of glucose and MeS on membrane potential

Figures 3(A) and 3(B) show examples of plasma membrane potential responses to glucose and MeS respectively in single
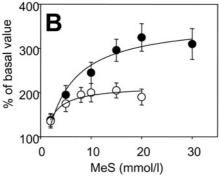
Figure 2   Effects of MeS concentration on insulin secretion and intracellular Ca^{2+} in rat islets and islet cells
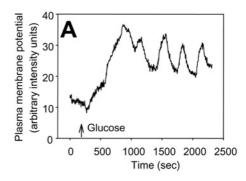
(**A**) Example of MeS-stimulated insulin secretion in a column perifusion of 50–80 rat islets. (**B**) Ca^{2+} measurement and insulin secretion were determined in single rat islet cells prepared by dispersion of whole islets. Average levels of Ca^{2+} (○) were determined as means $\pm$ S.E.M. from individual rat islet cells at each MeS concentration ($n = 58$). Insulin secretion over 30 min (●) was measured in 48-well plates under the same conditions as used for measurement of Ca^{2+}. Results are means $\pm$ S.E.M. for three independent experiments.

rat islet cells. Both fuels depolarized the plasma membrane, as indicated by an increase in signal. Superimposed on the depolarized membrane potential were similar oscillatory patterns induced by each fuel.

Both fuels also hyperpolarized the mitochondrial membrane potential. Increasing glucose from 4 to 10 mM caused an increase of $59 \pm 19\%$ ($n = 35$). An increase in MeS from 0 to 10 mM in the presence of 4 mM glucose caused a rise of $68 \pm 21\%$ ($n = 43$). Values are expressed as intensity units of TMRE fluorescence compared with basal values of 100%.

Effect of glucose and MeS on intracellular NAD(P)H and NAD(P) in rat and mouse islets

Figure 4(A) shows a comparison of whole-cell NAD(P)H/NAD(P) ratio responses using autofluorescence in a suspension of INS-1 cells. The response to MeS (first addition) was an immediate increase in NAD(P)H, whereas the response to glucose (second addition) was slightly delayed, but greater in magnitude. NAD(P)H was assessed in intact rat and mouse islets by two-photon excitation of intracellular NAD(P)H, which allows monitoring of intracellular single islet metabolism [23]. The NAD(P)H autofluorescence image in a rat islet in response to MeS is illustrated in Figure 4(B). Analysis of a series of such images showed that MeS caused a sustained increase in NAD(P)H autofluorescence in rat islets (Figure 4C), while it failed to significantly increase the NAD(P)H/NAD(P) ratio in mouse islets
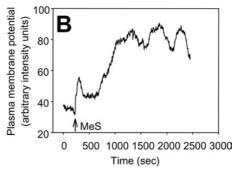

Figure 3   Illustration of plasma membrane potential ($\Delta\Psi$) oscillations in response to MeS (10 mm/l) and glucose (increase to 10 mm/l) in single rat islet cells

Cells were equilibrated with DiSBAC2(3) for 20 min and (**A**) glucose or (**B**) MeS was added as indicated by arrows. Experiments were repeated three (glucose) or four (MeS) times. An increase in the fluorescent signal indicates depolarization.

(Figure 4D). The magnitude of the change in response to glucose was greater than that with MeS. The order of addition of glucose and MeS did not significantly change the magnitude or lag of the responses.

Although two-photon excitation permits monitoring of live islet metabolism, the method does not distinguish between NADH and NADPH. We therefore measured individual nucleotides chemically in islet extracts using enzymatic recycling methods and expressed changes in the nucleotide levels as a ratio between the reduced form and the total (reduced plus oxidized forms). A summary of the changes in NADH and NADPH in rat and mouse islets in response to glucose and MeS (rat islets) is presented in Table 1. In rat islets, NADPH rose by 40% 1 min after MeS addition, whereas only a 20% increase occurred in response to glucose. This identifies NADPH as an early signal generated by MeS in rat islet cells. After 5 min, the rise in NADPH ratio due to MeS and glucose exposure reached similar values. The NADH to total (NAD + NADH) ratio was increased by both fuels after 1 min, by MeS somewhat more than by glucose. While the MeS-induced rise was considerably greater at 5 min, the glucose-dependent rise did not increase much more. Mouse islets responded in a similar manner to stimulatory glucose, except that the ratios were more reduced.

To test the possibility that the effect of MeS on NADPH might have an impact on secretion, we used Methylene Blue to lower cytosolic NADPH levels [29]. Methylene Blue inhibited MeS-stimulated secretion in rat islets, while KCl-induced secretion was not affected (Figure 5A). Importantly, Methylene Blue also diminished the depolarization of the plasma membrane caused by MeS without affecting the increment in KCl-induced depolarization (Figures 5B–5D).
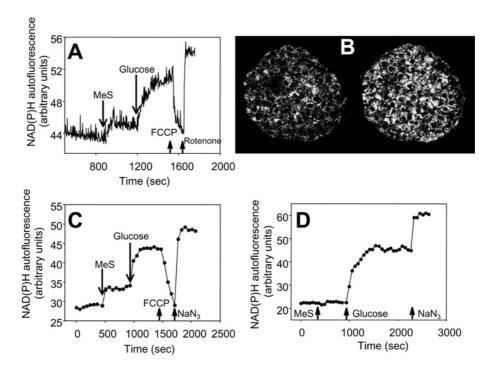
Figure 4   Effects of MeS and glucose on NAD(P)H autofluorescence in INS-1 cells and islets

Addition of 10 mmol/l MeS, 10 mmol/l glucose, 1 μmol/l FCCP, 1 μmol/l rotenone and 3 mmol/l NaN$_3$ are indicated by arrows, with fluorescence measured as described in the Materials and methods section. (**A**) Example of NAD(P)H responses in a population of INS-1 cells. (**B**) Example of the NAD(P)H image in a rat islet before (left) and after (right) MeS stimulation. Time-course of rat (**C**) and mouse (**D**) islet NAD(P)H responses to MeS and glucose. Islet data are illustrations from three independent experiments.

Table 1   Effects of glucose and MeS on NADH and NADPH levels in rat and mouse islets

Values are means $\pm$ S.E.M. for three to eight independent experiments. After overnight culture, islets were pre-incubated for 30 min at 4 mmol/l glucose, followed by incubation in the presence of the indicated fuel (10 mmol/l) for 1 or 5 min. Average values of NADH + NAD and NADPH + NADP were 0.48 $\pm$ 0.05 and 0.05 $\pm$ 0.005 pmol/islet respectively in rat islets. In mouse islets, NADPH + NADP averaged 0.042 $\pm$ 0 pmol/islet ($n = 17$). Control continued incubation in 4 mM glucose and did not change between 1 and 5 min. Control values are averages over both time points.

(a) Rat

	NADH/(NADH+NAD) ratio		NADPH/(NADPH+NADP) ratio	
Sample Time (min)...	1	5	1	5
Control	0.039 $\pm$ 0.003		0.51 $\pm$ 0.04	
Glucose	0.057 $\pm$ 0.004	0.065 $\pm$ 0.01	0.62 $\pm$ 0.04	0.71 $\pm$ 0.06
MeS	0.067 $\pm$ 0.01	0.097 $\pm$ 0.01	0.71 $\pm$ 0.04	0.70 $\pm$ 0.06

(b) Mouse

	NADPH/(NADPH+NADP) ratio	
Sample Time (min)...	1	5
Control	0.79 $\pm$ 0.03	
Glucose	0.93 $\pm$ 0.007	0.83 $\pm$ 0.10

Effect of glucose and MeS on the ATP/ADP ratio

Both glucose and MeS increased the ATP/ADP ratio nearly 2-fold in rat islets (Table 2), but MeS appeared to elicit a faster response that was maximal at 1 min, whereas the glucose response continued to increase over 5 min. In mouse islets, in contrast, the glucose-induced increase of nearly 2-fold in the ATP/ADP ratio peaked at 2 min, whereas MeS caused only a transient 30 % increase in the ATP/ADP ratio.

Malic enzyme activity

Measurement of malic enzyme activity in rat and mouse islets and INS-1 cells confirmed previous findings of MacDonald [17]. Homogenates of rat islets and INS-1 cells had activities of 235 $\pm$ 23 (islets) and 300 $\pm$ 21 (INS-1 cells) nmol of NADP converted into NADPH/min per mg of protein at 37 °C ($n = 3$). Activity in mouse islets was below the level of detection (0.6 nmol/min per mg of protein).

DISCUSSION

The mitochondrial substrate succinate, administered as MeS, can stimulate insulin secretion in rat islets, but it is generally ineffective in mouse islets [12,13,17,30]. The present studies were undertaken to determine and compare the key metabolic secretory signals generated by MeS and glucose in mouse and rat islets and to understand their differences. MeS, like glucose, elevated cytosolic free Ca²⁺, depolarized the plasma membrane, hyperpolarized the mitochondrial membrane potential, increased the cellular NAD(P)H/NAD(P) ratio and elevated the ATP/ADP ratio in rat, but not mouse, islets and islet cells. We propose that pyruvate and NADPH may be important common intermediates from MeS and glucose, but generated by somewhat different paths by the two fuels, and this may also account for the ineffectiveness of MeS in mouse islets. Thus succinate enters the mitochondria in exchange for malate via the dicarboxylate carrier (the mitochondrial malate being regenerated from metabolism of succinate though the succinate dehydrogenase and fumarase reactions), and the cytosolic malate is decarboxylated to pyruvate by malic enzyme together with the production of NADPH
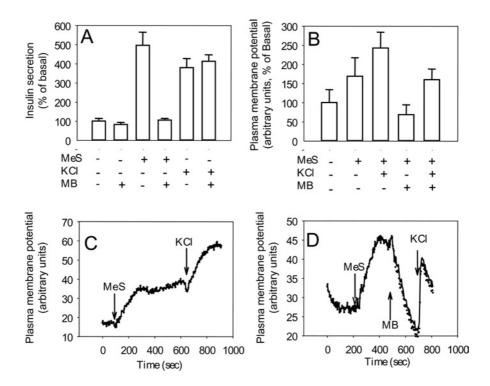
Figure 5   Effects of Methylene Blue on insulin secretion and plasma membrane potential in rat islets and islet cells

(**A**) Insulin secretion results are means ± S.E.M. for three independent experiments. (**B**) Plasma membrane potential results are means ± S.E.M. for four to eight independent measurements. Increased values indicate depolarization. (**C**, **D**) Representative examples of single rat islet cell responses. Additions of 10 mmol/l MeS, 25 mmol/l KCl and 10 μg/ml Methylene Blue (MB) are indicated by arrows.

Table 2   Effects of glucose and MeS on the ATP/ADP ratio in rat and mouse islets

Values are means ± S.E.M. for four independent experiments. Islets were prepared as described in Table 1. Control continued incubation in 4 mM glucose and did not change between 1 and 5 min. Control values are averages over all time points.

	ATP/ADP ratio (rat)			ATP/ADP ratio (mouse)		
Time (min) …	1	2	5	1	2	5
Glucose (4 mM)	4.4 ± 0.2			2.7 ± 0.1		
Glucose (10 mM)	6.7 ± 0.6	7.1 ± 0.4	8.1 ± 0.6	4.5 ± 0.2	5.2 ± 0.1	4.8 ± 0.3
MeS (10 mM)	8.1 ± 0.5	7.3 ± 0.3	7.2 ± 0.4	3.7 ± 0.3	3.4 ± 0.2	3.1 ± 0.2

(Figure 6). Additionally, the flow of malate into the cytosol may shift the malate dehydrogenase equilibrium there to generate NADH. Mouse islets have generally been shown to lack malic enzyme [17], a finding that we confirmed, and therefore they would not produce pyruvate and NADPH from MeS; hence, if these intermediates are important for stimulus–secretion coupling, this could explain the ineffectiveness of MeS as a secretagogue in that species.

There may be alternative pathways for NADPH production from glucose in the absence of malic enzyme. MacDonald [17] has suggested that this occurs via cytosolic isocitrate dehydrogenase, which is highly expressed in mouse, but not rat, islets. In addition, leucine plus glutamine give rise to α-oxoglutarate that can exchange for malate via the dicarboxylate carrier. Glutamate dehydrogenase, itself, is distributed between mitochondria and the cytosol and can use NADP as cofactor to generate NADPH in the cytosol. All anaplerotic fuels also promote citrate export and formation of malonyl-CoA.

We have shown previously that substances that support acetyl-CoA production and anaplerosis, including glucose and glutamine plus leucine [31], also generate malonyl-CoA, an important signal-generating intermediate in the β-cell [32–34]. The current studies support the concept that MeS is also anaplerotic as a consequence of malic enzyme activity and pyruvate generation in the cytosol. Without malic enzyme, succinate simply exchanges one tricarboxylic acid cycle intermediate, succinate, for another, malate, with no net anaplerosis. Thus it is expected that MeS would generate malonyl-CoA like other anaplerotic stimuli.

Glucose and MeS both increased the ATP/ADP ratio in rat islets, which would be expected to close K_{ATP} channels and therefore depolarize the plasma membrane and lead to a rise in cytosolic Ca^{2+}, as we have shown here. However, as found previously for glucose in both rat and mouse islets [4,6], the rise in Ca^{2+} concentration during MeS stimulation of rat islets did not correlate with the increase in secretion following a graded challenge with this fuel. This suggested that Ca^{2+} alone did not account for MeS-induced secretion, and that, like glucose, MeS-induced secretion includes a K_{ATP}-channel-independent component [4,6].

The major difference between glucose and MeS with regards to effects on intracellular Ca^{2+}, plasma membrane potential and
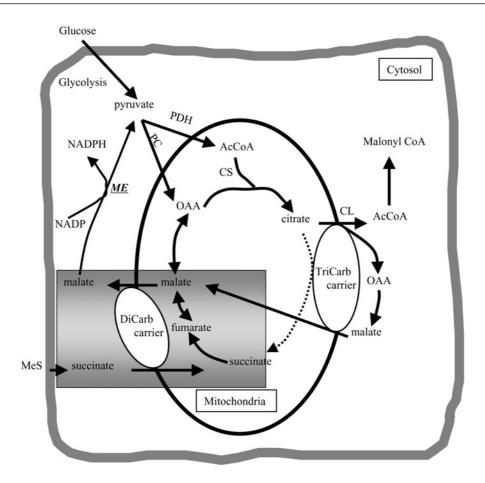
Figure 6   Illustration of mitochondrial carriers used by MeS

Succinate enters the mitochondrion on the dicarboxylate (DiCarb) carrier in exchange for malate. Malate can either be converted into pyruvate via malic enzyme (ME) or re-enter the mitochondrion via the tricarboxylate (TriCarb) carrier. AcCoA, acetyl-CoA; CL, citrate lyase; CS, citrate synthase; OAA, oxaloacetate; PC, pyruvate carboxylase; PDH, pyruvate dehydrogenase.

the ATP/ADP ratio in rat islets and islet cells was the lag, which was shorter with MeS than with glucose. The shorter lag can be explained by rapid entry of succinate into the tricarboxylic acid cycle, since it bypasses glycolysis and directly enters the mitochondria. The rise in the ATP/ADP ratio seen with MeS, which is to an extent similar to that with high glucose, is in agreement with reports on increased ATP levels after MeS challenge in rat β-cells [35] and INS-1 cells [36], but appears to be in contrast with a previous report from our laboratory, where MeS did not significantly increase ATP levels in rat islets [37]. In the latter case, the islet ATP content was measured as ATP-dependent luciferase activity in lysates of transient luciferase-expressing islets. The difference between protocols is that samples in the latter study were not deproteinized before ATP measurement [37], so it is probable that ongoing glycolysis may have restored the ATP in the high-glucose-containing samples. In the present study, islets were deproteinized, preventing further enzymatic generation of ATP.

Oscillatory metabolism is an important feature leading to oscillatory secretion in β-cells. The source of these oscillations and the mechanism of orchestration are unknown. We have shown that MeS and glucose caused similar oscillatory responses in Ca²⁺ and membrane potential in rat islets. The observation that a mitochondrial substrate, MeS, generated a similar pattern of oscillations as glucose suggests that systems other than glycolysis might control these oscillations. Indeed, oscillations in the activities of several enzymes and metabolites have been

demonstrated in mitochondrial fractions of INS-1 cells [38]. This suggests a possibility that all metabolism might oscillate, and the pacemaker activity is a result of multiple factors. However, another possibility is that oscillations in the activity of PFK might be triggered without stimulatory glucose, as follows. The rise in cytosolic NADH caused by MeS may inhibit glyceraldehyde-3-phosphate dehydrogenase, leading to a rise in triose phosphates and hence fructose 1,6-bisphosphate into the range necessary to trigger a burst of PFK activity and glycolytic oscillations [39]. Previously, stimulation of Ca²⁺ and insulin secretion by MeS was reported to be dependent on the presence of substimulatory levels of glucose [40].

Our observation that Ca²⁺ responses reached a maximum while secretion still increased with increasing MeS (Figure 2A) suggests additional putative secretory signals. To compare effects of glucose and MeS on NADH and NADPH, we measured changes in their combined responses in populations of single cells (INS-1) and whole rat islets following single- and two-photon excitation of NAD(P)H. Although neither method allowed us to distinguish between NADPH and NADH, owing to their identical spectral characteristics, two-photon excitation has proven to be useful for non-invasive monitoring of islet metabolism for prolonged time periods. Consistent with previous reports using glucose [23], increases in whole-islet autofluorescence occurred within 30 s of fuel addition. The total glucose-dependent rise in the NAD(P)H signal was larger than that due to MeS, but the chemical measurement of nucleotides showed a different pattern. Although

levels of NADPH due to each fuel reached similar values after 5 min, MeS increased NADH to a considerably greater extent than glucose after 5 min of exposure.

The apparent difference between results obtained by measurement of total NAD(P)H autofluorescence in cells and islets and chemical measurement of NADH and NADPH can be explained by greater autofluorescence of mitochondrial NAD(P)H due to the enhanced fluorescence of mitochondrial protein-bound NAD(P)H [13,17,41]. Thus glucose had a greater effect on mitochondrial NADH, resulting in a greater autofluorescence signal. The disproportionate effect of MeS on the assayed NADH suggests that MeS increased the cytoplasmic pool of NADH to a greater extent than glucose. This would be expected because succinate exchange for malate would lead to high levels of cytosolic malate, and the presence of malate dehydrogenase in the cytosol would catalyse conversion of some of the malate into oxaloacetate with production of NADH. An additional explanation may be that NADH generated from glucose is transported into the mitochondria by both malate–aspartate and α-glycerophosphate shuttles, whereas that produced from malate may use only the malate–aspartate shuttle because of a lower level of dihydroxyacetone phosphate at basal glucose. It is not known if this increase in cytosolic NADH has an impact on signalling in β-cells as in other cell types [42,43].

The fact that the early elevation of NADPH (maximum at 1 min) by MeS correlated with or even preceded the Ca^{2+} rise in single rat islet cells supports a potential role of this putative messenger in secretion, as previously suggested by Ivarsson et al. [44]. Chemical measurement of nucleotides allowed us to evaluate early changes in generation of both NADPH and NADH. The MeS-dependent rise in NADPH peaked before that of NADH, consistent with preferential conversion by cytosolic malic enzyme of malate plus NADP into pyruvate plus NADPH. Increases in NADH and NADPH in response to glucose are in good agreement with previously published data in rat islets [45]. Generation of NADPH occurs predominantly in the cytosolic compartment [46]. Compounds that inhibit the formation of cytosolic NADPH, such as nicotinic acid and Methylene Blue, have been shown to inhibit insulin secretion in clonal β-cells [47] and rat pancreatic islets [48]. In accordance with these reports, our data show that MeS-dependent secretion and plasma membrane depolarization are inhibited by Methylene Blue. In contrast, KCl-dependent secretion and depolarization were not affected by Methylene Blue treatment, demonstrating that the effect of this compound was restricted to metabolically induced depolarization.

Although the precise role of cytosolic NADPH in fuel signalling in β-cells has not been fully elucidated, recent studies have demonstrated that the intracellular addition of NADPH directly stimulates exocytosis of insulin granules, an effect that was proposed to be mediated by glutaredoxin and thioredoxin [44]. In addition, NADPH might also play a role in the regulation of the activity of Kv2.1 channels [49], a putative major contributor to voltage-dependent outward K^+ current in insulinoma cells and rodent pancreatic β-cells [50]. Kv channels, identified in the plasma membrane of β-cells [49], are involved in plasma membrane repolarization during fuel stimulation, and thus may contribute to the maintenance of the oscillatory pattern of β-cell metabolism and secretion. It is possible that oscillations in cytosolic NADPH might directly modulate Kv2.1 channels and thus contribute to oscillations in the plasma membrane. It can be seen in our experiments (Figure 5C compared with Figure 5D) that pre-treatment with Methylene Blue shortened KCl-induced depolarization, an effect that could be explained by the activation of the Kv channels and therefore a more transient depolarization

of the cell. These data are consistent with the reported closure of Kv channels by cytosolic NADPH [51].

Our results generally agree with others in the literature [12,13,17,30] and with the data from the group of Tamarit-Rodriguez [40] that demonstrated that the maximum secretory responses to glucose and MeS were indistinguishable in rat islets. However, in the latter study, both glucose and MeS also elevated the intracellular Ca^{2+} concentration in Swiss OF1 mouse islets and induced similar patterns of oscillations. The oscillations reported in that study were 'fast' oscillations, most likely to be due to Ca^{2+} bursting, in contrast with 'slow' oscillations shown in the present study which may reflect metabolic processes. In contrast with those findings, we did not find an increase in either Ca^{2+} or secretion with MeS in Swiss–Webster mouse islet cells. This is in agreement with the data from MacDonald [17], who documented no MeS-stimulated insulin secretion or malic enzyme activity in C57Bl, NSA, BALBc or ICR mice. However, it was also shown that MIN-6 and βTC-7 mouse cell lines expressed malic enzyme [17], thus indicating that some mouse models may express this enzyme while most do not. It is not known whether the Swiss OF1 mice express malic enzyme.

In summary, our data showing very similar patterns of the metabolically generated signals, increased ATP/ADP, NAD(P)H and Ca^{2+} as well as depolarization of the plasma membrane and hyperpolarization of the mitochondrial potentials, with glucose and MeS in rat, but not mouse, islets are consistent with the common intermediates being pyruvate, cytosolic NADPH or both. The data suggest that MeS generates these critical common intermediates via malic enzyme, which is not expressed in islets from most mouse strains. Information in the literature supports the importance of both molecules, since lowering NADPH in the cytosol inhibits secretion, while methyl pyruvate stimulates insulin secretion in most models tested. Further studies are underway to compare methyl pyruvate with glucose and MeS in rat and mouse islets and to determine the effect of malic enzyme expression on secretion in mice.

REFERENCES

1   Matschinsky, F. M. (1996) Banting Lecture 1995. A lesson in metabolic regulation inspired by the glucokinase glucose sensor paradigm. Diabetes **45**, 223–241

2   Malaisse, W. J., Sener, A., Herchuelz, A. and Hutton, J. C. (1979) Insulin release: the fuel hypothesis. Metab. Clin. Exp. **28**, 373–386

3   Misler, S., Barnett, D. W., Gillis, K. D. and Pressel, D. M. (1992) Electrophysiology of stimulus-secretion coupling in human β-cells. Diabetes **41**, 1221–1228

4   Heart, E., Corkey, R. F., Wikstrom, J. D., Shirihai, O. S. and Corkey, B. E. (2006) Glucose-dependent increase in mitochondrial membrane potential, but not cytoplasmic calcium, correlates with insulin secretion in single islet cells. Am. J. Physiol. Endocrinol. Metab. **290**, E143–E148

5   Gembal, M., Detimary, P., Gilon, P., Gao, Z. Y. and Henquin, J. C. (1993) Mechanisms by which glucose can control insulin release independently from its action on adenosine triphosphate-sensitive K^+ channels in mouse β cells. J. Clin. Invest. **91**, 871–880

6   Ravier, M. A. and Henquin, J. C. (2002) Time and amplitude regulation of pulsatile insulin secretion by triggering and amplifying pathways in mouse islets. FEBS Lett. **530**, 215–219

7   Tornheim, K. (1997) Are metabolic oscillations responsible for normal oscillatory insulin secretion? Diabetes **46**, 1375–1380

8   Yaney, G. C., Schultz, V., Cunningham, B. A., Dunaway, G. A., Corkey, B. E. and Tornheim, K. (1995) Phosphofructokinase isozymes in pancreatic islets and clonal β-cells (INS-1). Diabetes **44**, 1285–1289

9   O'Rahilly, S., Turner, R. C. and Matthews, D. R. (1988) Impaired pulsatile secretion of insulin in relatives of patients with non-insulin-dependent diabetes. N. Engl. J. Med. **318**, 1225–1230

10 Prentki, M. and Matschinsky, F. M. (1987) Ca^{2+}, cAMP, and phospholipid-derived messengers in coupling mechanisms of insulin secretion. Physiol. Rev. **67**, 1185–1248

11 MacDonald, M. J. (1993) Metabolism of the insulin secretagogue methyl succinate by pancreatic islets. Arch. Biochem. Biophys. **300**, 201–205

12 Malaisse, W. J., Rasschaert, J., Villanueva-Penacarrillo, M. L. and Valverde, I. (1993) Respiratory, ionic, and functional effects of succinate esters in pancreatic islets. Am. J. Physiol. **264**, E428–E433

13 MacDonald, M. J., Fahien, L. A., Mertz, R. J. and Rana, R. S. (1989) Effect of esters of succinic acid and other citric acid cycle intermediates on insulin release and inositol phosphate formation by pancreatic islets. Arch. Biochem. Biophys. **269**, 400–406

14 Ashcroft, S. J. H. and Christie, M. R. (1979) Effects of glucose on the cytosolic ratio of reduced/oxidized nicotinamide–adenine dinucleotide phosphate in rat islets of Langerhans. Biochem. J. **184**, 697–700

15 MacDonald, M. J. (2003) Export of metabolites from pancreatic islet mitochondria as a means to study anaplerosis in insulin secretion. Metab. Clin. Exp. **52**, 993–998

16 MacDonald, M. J., Fahien, L. A., Brown, L. J., Hasan, N. M., Buss, J. D. and Kendrick, M. A. (2005) Perspective: emerging evidence for signaling roles of mitochondrial anaplerotic products in insulin secretion. Am. J. Physiol. Endocrinol. Metab. **288**, E1–E15

17 MacDonald, M. J. (2002) Differences between mouse and rat pancreatic islets: succinate responsiveness, malic enzyme, and anaplerosis. Am. J. Physiol. Endocrinol. Metab. **283**, E302–E310

18 de Vargas, L. M., Sobolewski, J., Siegel, R. and Moss, L. G. (1997) Individual β cells within the intact islet differentially respond to glucose. J. Biol. Chem. **272**, 26573–26577

19 Berts, A., Gylfe, E. and Hellman, B. (1995) Ca^{2+} oscillations in pancreatic islet cells secreting glucagon and somatostatin. Biochem. Biophys. Res. Commun. **208**, 644–649

20 Farfari, S., Schulz, V., Corkey, B. and Prentki, M. (2000) Glucose-regulated anaplerosis and cataplerosis in pancreatic β-cells: possible implication of a pyruvate/citrate shuttle in insulin secretion. Diabetes **49**, 718–726

21 Grynkiewicz, G., Poenie, M. and Tsien, R. Y. (1985) A new generation of calcium indicators with greatly improved flourescence properties. J. Biol. Chem. **260**, 3440–3450

22 Pralong, W. F., Bartley, C. and Wollheim, C. B. (1990) Single islet β-cell stimulation by nutrients: relationship between pyridine nucleotides, cytosolic Ca^{2+} and secretion. EMBO J. **9**, 53–60

23 Bennett, B. D., Jetton, T. L., Ying, G., Magnuson, M. A. and Piston, D. W. (1996) Quantitative subcellular imaging of glucose metabolism within intact pancreatic islets. J. Biol. Chem. **271**, 3647–3651

24 Lowry, O. H., Passonneau, J. V., Schulz, D. W. and Rock, M. K. (1961) The measurement of pyridine nucleotides by enzymatic cycling. J. Biol. Chem. **236**, 2746–2755

25 Kato, T., Berger, S. J., Carter, J. A. and Lowry, O. H. (1973) An enzymatic cycling method for nicotinamide-adenine dinucleotide with malic and alcohol dehydrogenases. Anal. Biochem. **53**, 86–97

26 Cunningham, B. A., Richard, A. M., Dillon, J. S., Daley, J. T., Civelek, V. N., Deeney, J. T., Yaney, G. C., Corkey, B. E. and Tornheim, K. (2003) Glucagon-like peptide 1 and fatty acids amplify pulsatile insulin secretion from perifused rat islets. Biochem. J. **369**, 173–178

27 Deeney, J. T., Kohler, M., Kubik, K., Brown, G., Schultz, V., Tornheim, K., Corkey, B. E. and Berggren, P. O. (2001) Glucose-induced metabolic oscillations parallel those of Ca^{2+} and insulin release in clonal insulin-secreting cells: a multiwell approach to oscillatory cell behavior. J. Biol. Chem. **276**, 36946–36950

28 Liu, Y. Q., Tornheim, K. and Leahy, J. L. (1999) Glucose–fatty acid cycle to inhibit glucose utilization and oxidation is not operative in fatty acid-cultured islets. Diabetes **48**, 1747–1753

29 Ammon, H. P. and Verspohl, E. J. (1979) Effect of Methylene Blue on pyridine nucleotides and insulin secretion of rat pancreatic islets. Diabetologia **17**, 41–44

30 Zawalich, W. S., Zawalich, K. C., Cline, G., Shulman, G. and Rasmussen, H. (1993) Comparative effects of monomethylsuccinate and glucose on insulin secretion from perifused rat islets. Diabetes **42**, 843–850

31 Prentki, M., Vischer, S., Glennon, M. C., Regazzi, R., Deeney, J. T. and Corkey, B. E. (1992) Malonyl-CoA and long chain acyl-CoA esters as metabolic coupling factors in nutrient-induced insulin secretion. J. Biol. Chem. **267**, 5802–5810

32 Prentki, M. and Corkey, B. E. (1996) Are the β-cell signaling molecules malonyl-CoA and cystolic long-chain acyl-CoA implicated in multiple tissue defects of obesity and NIDDM? Diabetes **45**, 273–283

33 Brun, T., Roche, E., Assimacopoulos-Jeannet, F., Corkey, B. E., Kim, K. H. and Prentki, M. (1996) Evidence for an anaplerotic/malonyl-CoA pathway in pancreatic β-cell nutrient signaling. Diabetes **45**, 190–198

34 Corkey, B. E., Glennon, M. C., Chen, K. S., Deeney, J. T., Matschinsky, F. M. and Prentki, M. (1989) A role for malonyl-CoA in glucose-stimulated insulin secretion from clonal pancreatic β-cells. J. Biol. Chem. **264**, 21608–21612

35 Ishihara, H., Maechler, P., Gjinovci, A., Herrera, P. L. and Wollheim, C. B. (2003) Islet β-cell secretion determines glucagon release from neighbouring α-cells. Nat. Cell Biol. **5**, 330–335

36 Maechler, P., Kennedy, E. D., Wang, H. and Wollheim, C. B. (1998) Desensitization of mitochondrial Ca^{2+} and insulin secretion responses in the β cell. J. Biol. Chem. **273**, 20770–20778

37 Alarcon, C., Wicksteed, B., Prentki, M., Corkey, B. E. and Rhodes, C. J. (2002) Succinate is a preferential metabolic stimulus-coupling signal for glucose-induced proinsulin biosynthesis translation. Diabetes **51**, 2496–2504

38 MacDonald, M. J., Fahien, L. A., Buss, J. D., Hasan, N. M., Fallon, M. J. and Kendrick, M. A. (2003) Citrate oscillates in liver and pancreatic β cell mitochondria and in INS-1 insulinoma cells. J. Biol. Chem. **278**, 51894–51900

39 Tornheim, K. and Lowenstein, J. M. (1975) The purine nucleotide cycle: control of phosphofructokinase and glycolytic oscillations in muscle extracts. J. Biol. Chem. **250**, 6304–6314

40 Mukala-Nsengu, A., Fernandez-Pascual, S., Martin, F., Martin-del-Rio, R. and Tamarit-Rodriguez, J. (2004) Similar effects of succinic acid dimethyl ester and glucose on islet calcium oscillations and insulin release. Biochem. Pharmacol. **67**, 981–988

41 Ince, C., Coremans, J. M. and Bruining, H. A. (1992) In vivo NADH fluorescence. Adv. Exp. Med. Biol. **317**, 277–296

42 Suzuki, Y. J. and Ford, G. D. (1999) Redox regulation of signal transduction in cardiac and smooth muscle. J. Mol. Cell. Cardiol. **31**, 345–353

43 Kim, M. Y., Zhang, T. and Kraus, W. L. (2005) Poly(ADP-ribosyl)ation by PARP-1: 'PAR-laying' NAD^{+} into a nuclear signal. Genes Dev. **19**, 1951–1967

44 Ivarsson, R., Quintens, R., Dejonghe, S., Tsukamoto, K., in 't Veld, P., Renstrom, E. and Schuit, F. C. (2005) Redox control of exocytosis: regulatory role of NADPH, thioredoxin, and glutaredoxin. Diabetes **54**, 2132–2142

45 Trus, M. D., Warner, H. and Matschinsky, F. M. (1980) Effects of glucose on insulin release and on intermediary metabolism of isolated perifused pancreatic islets from fed and fasted rats. Diabetes **29**, 1–14

46 Sener, A., Malaisse-Lagae, F., Dufrane, S. P. and Malaisse, W. J. (1984) The coupling of metabolic to secretory events in pancreatic islets: the cytosolic redox state. Biochem. J. **220**, 433–440

47 Ammon, H. P., Akhtar, M. S., Grimm, A. and Niklas, H. (1979) Effect of methylene blue and thiol oxidants on pancreatic islet GSH/GSSG ratios and tolbutamide mediated insulin release in vitro. Naunyn Schmiedebergs Arch. Pharmacol. **307**, 91–96

48 Salgado, A. P., Pereira, F. C., Seica, R. M., Fernandes, A. P., Flatt, P. R., Santos, R. M., Rosario, L. M. and Ramasamy, R. (1999) Modulation of glucose-induced insulin secretion by cytosolic redox state in clonal β-cells. Mol. Cell. Endocrinol. **154**, 79–88

49 MacDonald, P. E. and Wheeler, M. B. (2003) Voltage-dependent K^{+} channels in pancreatic β cells: role, regulation and potential as therapeutic targets. Diabetologia **46**, 1046–1062

50 MacDonald, P. E., Ha, X. F., Wang, J., Smukler, S. R., Sun, A. M., Gaisano, H. Y., Salapatek, A. M., Backx, P. H. and Wheeler, M. B. (2001) Members of the Kv1 and Kv2 voltage-dependent K^{+} channel families regulate insulin secretion. Mol. Endocrinol. **15**, 1423–1435

51 MacDonald, P. E., Sewing, S., Wang, J., Joseph, J. W., Smukler, S. R., Sakellaropoulos, G., Saleh, M. C., Chan, C. B., Tsushima, R. G., Salapatek, A. M. and Wheeler, M. B. (2002) Inhibition of Kv2.1 voltage-dependent K^{+} channels in pancreatic β-cells enhances glucose-dependent insulin secretion. J. Biol. Chem. **277**, 44938–44945